Research Article

Rapid Communications in Mass Spectrometry

Received: 27 April 2016 Revised: 14 June 2016 Accepted: 15 June 2016 Published online in Wiley Online Library

Rapid Commun. Mass Spectrom. **2016**, *30*, 1835–1845
(wileyonlinelibrary.com) DOI: 10.1002/rcm.7667

Diisopropylethylamine/hexafluoroisopropanol-mediated ion-pairing ultra-high-performance liquid chromatography/mass spectrometry for phosphate and carboxylate metabolite analysis: utility for studying cellular metabolism

Lili Guo[1], Andrew J. Worth[1], Clementina Mesaros[1], Nathaniel W. Snyder[2], Jerry D. Glickson[3] and Ian A. Blair[1]*

[1]Penn SRP and Center for Excellence in Environmental Toxicology, Department of Systems Pharmacology and Translational Therapeutics, University of Pennsylvania, Philadelphia, PA 19104, USA
[2]A.J. Drexel Autism Institute, Drexel University, Philadelphia, PA 19104, USA
[3]Department of Radiology, Perelman School of Medicine, University of Pennsylvania, Philadelphia, PA 19104, USA

RATIONALE: Mass spectrometric (MS) analysis of low molecular weight polar metabolites can be challenging because of poor chromatographic resolution of isomers and insufficient ionization efficiency. These metabolites include intermediates in key metabolic pathways, such as glycolysis, the pentose phosphate pathway, and the Krebs cycle. Therefore, sensitive, specific, and comprehensive quantitative analysis of these metabolites in biological fluids or cell culture models can provide insight into multiple disease states where perturbed metabolism plays a role.
METHODS: An ion-pairing reversed-phase ultra-high-performance liquid chromatography (IP-RP-UHPLC)/MS approach to separate and analyze biochemically relevant phosphate- and carboxylic acid-containing metabolites was developed. Diisopropylethylamine (DIPEA) was used as an IP reagent in combination with reversed-phase liquid chromatography (RP-LC) and a triple quadrupole mass spectrometer using selected reaction monitoring (SRM) and negative electrospray ionization (NESI). An additional reagent, hexafluoroisopropanol (HFIP), which has been previously used to improve sensitivity of nucleotide analysis by UHPLC/MS, was used to enhance sensitivity.
RESULTS: HFIP versus acetic acid, when added with the IP base, increased the sensitivity of IP-RP-UHPLC/NESI-MS up to 10-fold for certain analytes including fructose-1,6-bisphosphate, phosphoenolpyruvate, and 6-phosphogluconate. It also improved the retention of the metabolites on a C_{18} reversed-phase column, and allowed the chromatographic separation of important isomeric metabolites. This methodology was amenable to quantification of key metabolites in cell culture experiments. The applicability of the method was demonstrated by monitoring the metabolic adaptations resulting from rapamycin treatment of DB-1 human melanoma cells.
CONCLUSIONS: A rapid, sensitive, and specific IP-RP-UHPLC/NESI-MS method was used to quantify metabolites from several biochemical pathways. IP with DIPEA and HFIP increased the sensitivity and improved chromatographic separation when used with reversed-phase UHPLC.

Ultra-high-performance liquid chromatography/selected reaction monitoring mass spectrometry (UHPLC/SRM-MS) is considered to be the "gold standard" for quantification of relatively low abundance metabolites from complex biological matrices.[1] Robust and reproducible UHPLC/SRM-MS methods are dependent on several factors, including adequate and consistent chromatography, particularly for isomeric compounds, which are often indistinguishable by SRM/MS analysis. Efficient ionization in the source of the mass spectrometer is required for the detection of analytes. These requirements are particularly important when analyses are performed on complex biological samples, as co-eluting of interfering compounds can suppress signal and diminish the sensitivity, and potentially specificity, of a method.[2,3]

Cellular metabolism has received renewed interest in recent years due to emerging applications of metabolomics in drug discovery and precision medicine[4–6] and playing a causative role in a range of diseases.[7–11] In particular, the metabolic reprogramming that occurs in cancer has been proposed as contributing to pathogenesis, disease progression, and has sparked renewed interest in targeting altered metabolic pathways as therapeutic interventions.[12,13] As such, an improved understanding of cancer metabolism, as well as the genetic or epigenetic factors that contribute to the metabolic alterations, is critical to explore disease-specific phenotypes or pathways for therapeutic purposes. Unfortunately, many of these bioenergetic processes of interest involve metabolites that are difficult to analyze by

* *Correspondence to*: I. A. Blair, Center for Cancer Pharmacology, University of Pennsylvania, 854 BRB II/III, 421 Curie Boulevard, Philadelphia, PA 19104-6160, USA. E-mail: ianblair@mail.med.upenn.edu

conventional LC/SRM-MS approaches.[14–16] More specifically, glycolysis, the pentose phosphate pathway (PPP), and the Krebs or tricarboxylic acid (TCA) cycle are major metabolic pathways which can be differentially regulated by disease states.[11] Many of the metabolites are low molecular weight hydrophilic compounds, containing phosphate, carboxylic acid, or amino acid moieties. Therefore, retention on common reversed-phase C_8 or C_{18} LC columns is generally poor and many of the metabolites are not amenable to sensitive analysis by positive mode electrospray ionization (PESI). Metabolite concentrations can span a very wide concentration range and there are numerous isomeric metabolites. This means that accurate quantification requires selective and reproducible chromatography coupled with efficient generation of ions in the electrospray ionization source for quantification of low-abundance metabolites.

Many LC/MS methods for the analysis of small molecule polar metabolites have employed hydrophobic interaction liquid chromatography (HILIC)-mediated separation.[17–20] Advances in the materials for HILIC columns make this approach much more reliable than the earlier generation of columns. A drawback of this methodology is the necessity for sample resuspension in an organic solvent, which decreases sensitivity since some metabolites have very low solubility in high-organic solvents thus causing selective undervaluation. Using lower organic concentrations for the resuspension solvent impairs the binding of the analytes to the stationary phase of HILIC columns and causes peak shapes to be non-ideal, which then adds to the difficulty of separating isobaric or isomeric species. Moreover, relatively long equilibration times are required when using HILIC methods in order to obtain a stable retention time between runs.[21,22]

There are several reports detailing the chromatographic separation of polar metabolites using ion-pairing (IP)-LC/MS.[23–30] The exact mechanism of IP-LC is still controversial even though it was discovered over 30 years ago.[31,32] A widely accepted mechanism involves an ion pair model in which the hydrophobic moieties of an IP non-nucleophilic base (such as tributylamine) interact with the hydrophobic groups (such as C_{18}) on the stationary phase. Polar, negatively charged metabolites such as phosphates and carboxylates then interact with the protonated nitrogen moiety of the tributylamine base and are retained on the column.[25] The mobile phase is normally maintained at pH 7.0 in order to facilitate NESI and maximize interactions of the analyte with the immobilized IP reagent. Increasing the organic solvent content of the mobile phase (by gradient elution) reduces the interaction of the IP base with the stationary phase and allows the metabolites to elute from the column. The added non-nucleophilic base also serves to reduce the sodium and potassium adducts which can reduce the signal derived from the deprotonated analyte molecule $[M–H]^-$.[33,34]

Oligonucleotide analysis by IP-LC/MS has generally involved the addition of HFIP to the non-nucleophilic amine base in the mobile phase.[35] By titrating the base to near neutral pH with HFIP (pH 8), the phosphate-rich negatively charged oligonucleotides undergo IP with the positively charged base, resulting in increased chromatographic retention on reversed-phase LC columns.[33,34] In addition, the low boiling point of HFIP (58.2°C) facilitates its rapid evaporation from the surface of liquid droplets in the source of the mass spectrometer (Fig. 1). This process is hypothesized to rapidly increase the pH within the droplets due to the effective concentration of base, making this approach highly efficient in negative mode ionization.[35] As this approach is very effective for oligonucleotide analysis,[34,35] we reasoned that it should also be useful for the analysis of the phosphate- and carboxylic acid-containing small molecules that make up intermediary cellular metabolism. The negatively charged phosphate and carboxylate moieties on the metabolites should have similar chromatographic properties to oligonucleotides. To extend the analytical coverage of carbon metabolism, we also coupled IP with chemical derivatization in order to analyze isomeric phosphate metabolites as well as the unstable and poorly ionized[36,37] keto-acids α-ketoglutarate, pyruvate, and oxaloacetate metabolites.

EXPERIMENTAL

Chemicals and reagents

Diisopropylethylamine (DIPEA), tributylamine (TBA), 1,1,1,3,3,3-hexafluoro-2-propanol (HFIP), phenylhydrazine HCl, dimethyl sulfoxide (DMSO), rapamycin, glucose 6-phosphate, fructose 6-phosphate, mannose 6-phosphate, glucose 1-phosphate, mannose 1-phosphate, galactose 1-pohsphate, fructose 1,6-bisphosphate, glyceraldehyde 3-phosphate, dihydroxyacetone phosphate, 2-phosphoglycerate,

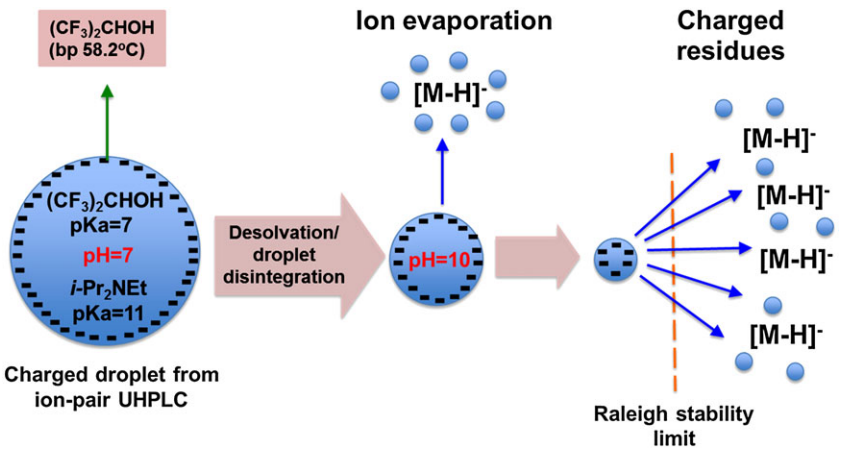

Figure 1. Scheme showing how HFIP facilitates NESI.

Rapid Communications in Mass Spectrometry

phosphoenolpyruvate, pyruvate, 6-phosphogluconate, ribulose 5-phosphate, ribose 5-phosphate, sedoheptulose 7-phosphate, erythrose 4-phosphate, glutathione, flavin adenine dinucleotide (FAD), nicotinamide adenine dinucleotide (NAD), NADH, nicotinamide adenine dinucleotide phosphate (NADP), NADPH, acetyl-CoA, succinyl-CoA, citrate, isocitrate, succinate, fumarate, malate, lactate, α-ketoglutarate, 2-hydroxyglutarate, oxaloacetate, acetoacetate, β-hydroxybutyrate, mevalonate, hexosamine-6-phosphate, phosphoserine, serine, glutamate, aspartate, AMP (adenosine monophosphate), ADP (adenosine diphosphate), ATP (adenosine triphosphate), CTP (cytidine triphosphate), UTP (uridine triphosphate), GTP (guanosine triphosphate), phosphohydroxypyruvic acid, acetyl-CoA, succinyl-CoA, [$^{13}C_5$,^{15}N]-glutamate, [$^{13}C_4$]-succinate, [$^{13}C_3$]-lactate and [$^{13}C_6$]-citrate were purchased from Sigma-Aldrich (St. Louis, MO, USA). Optima LC-MS grade water, methanol, and acetonitrile (ACN) were purchased from Thermo Fisher Scientific (Waltham, MA, USA). [$^{13}C_6$]-Glucose 6-phosphate, [$^{13}C_6$]-glucose, [$^{13}C_5$,$^{15}N_2$]-glutamine, [$^{13}C_4$,^{15}N]-aspartate, [$^{13}C_3$]-pyruvate, [$^{13}C_4$]-fumarate and glutathione ([$^{13}C_2$,^{15}N]-glycine) were purchased from Cambridge Isotope Laboratories (Tewksbury, MA, USA).

Standard solutions

Each standard compound or internal standard was weighed and dissolved by sonication in Optima pure water to stock solutions of 1 μg/mL. Initially, each of the compounds was run individually to check for interferences and determine the order of elution for isomeric compounds. The final standard solution mix contained 60 polar metabolites (Table 1) at a concentration of 1000 ng/mL. For quantification, a 10-point calibration curve was constructed by 1:2 serial dilutions from the highest concentration of calibration mixture with water. The stock solutions were kept at −20°C. Internal standard mixtures were made for each experiment in order to match the estimated amounts of the individual metabolites in the samples.

Cell culture, treatment and isotopic labeling

DB-1 melanoma cells were maintained in MEMα medium with 10% fetal bovine serum (FBS) and antibiotics (100 units/mL penicillin and 100 mg/L streptomycin). For the labeling experiment, DB-1 cells were cultured in 10 cm tissue culture plates, and incubated overnight with glucose- and glutamine-free DMEM containing 10% FBS as well as 5 mM [$^{13}C_6$]-glucose and 2 mM [$^{13}C_5$,$^{15}N_2$]-glutamine or corresponding unlabeled nutrients at the same concentrations. Human diffuse large cell lymphoma DLCL2 cells were maintained in RPMI medium containing 10% FBS and antibiotics. DLCL2 cells (2×10^6), cultured in tissue culture flasks, were incubated with 0.1% DMSO or 200 nM rapamycin for 48 h. Cells were counted at the end of each treatment. All treatments were performed in triplicate.

Metabolite extraction and derivatization

Cells were washed twice with phosphate-buffered saline (Mediatech, Manassas, VA, USA) (1 mM pH 7.4) before being scraped into 750 μL of ice-cold methanol/water (4/1 v/v). For cells treated with rapamycin, samples were spiked with internal standards (500 ng [$^{13}C_4$]-succinate, 500 ng [$^{13}C_6$]-citrate, 500 ng [$^{13}C_3$]-pyruvate, 2 μg [$^{13}C_3$]-lactate, 500 ng [$^{13}C_4$,^{15}N]-aspartate, 2 μg [$^{13}C_5$,^{15}N]-glutamate and 500 ng [$^{13}C_6$]-glucose 6-phosphate). Samples were pulse-sonicated for for 30 s with a probe tip sonicator and centrifuged at 16,000 *g* for 10 min. The supernatant was transferred to two new tubes: 50 μL were transferred to one tube and diluted 5 times with 50 mM ammonium carbonate for direct analysis of the underivatized redox cycling metabolites (Fig. 2) and 700 μL were transferred to one tube containing 300 μL of phenylhydrazine in methanol/water (4/1 v/v) (3 mg/mL) for analysis of underivatized and derivatized metabolites (Fig. 2). Derivatization was conducted by incubation at room temperature for 2 h before evaporation to dryness under nitrogen. Water (100 μL) was used to re-suspend the samples. Injection volume was 5 μL in both methods. The phenylhydrazine-derivatized samples were run with gradient 1 and the underivatized samples were run with gradient 2.

Ultra-high-performance liquid chromatography-mass spectrometry

An UltiMate 3000 quaternary UHPLC system equipped with a refrigerated autosampler (6°C) and a column heater was used. Both gradients used a Phenomenex Synergy Polar-RP column (150 × 2 mm i.d., 4 μm, 80 Å; Phenomenex, Torrance, CA, USA) at a flow rate of 0.2 mL/min. Solvent A was 5 mM DIPEA and 200 mM HFIP and solvent B was methanol with 5 mM DIPEA 200 mM HFIP. The linear gradient 1 was as follows: 100% A for 6 min, 98% A at 8 min, 86% A at 12 min, 50% A at 14 min and 10% A at 15 min. 10% A was held for 4 min, back to 100% A over 1 min prior to a 5 min equilibration. Linear gradient 2 was shorter, in order to run the unstable redox cycling metabolites (NAD^+, NADH, $NADP^+$ and NADPH) as quickly as possible after the extractions: 100% A for 2 min, 80% A at 4 min, 10% A at 6 min, and 10% A at 8 min. 10% A was held for 2 min, back to 100% A over 1 min prior to a 4 min equilibration. The separations were performed at 55°C. MS analysis was conducted on a TSQ Quantum Ultra AM mass spectrometer (Thermo Scientific, San Jose, CA, USA) equipped with a HESI II source operating in negative mode. The TSQ Quantum operating conditions were as follows: spray voltage 4000 V; vaporizer temperature 200°C; capillary temperature 350°C; tube lens 90 V. The sheath gas (nitrogen) and auxiliary gas (nitrogen) pressures were 45 and 10 (arbitrary units), respectively. Both Q1 and Q3 resolutions were set at 0.7 amu. Scan width was 0.002 and the dwell time was 20 ms. Collision-induced dissociation used argon as the collision gas at 1.5 mTorr. The collision energy was optimized for each metabolite and the values are reported in Table 1. Data analysis was performed with Xcalibur software (version 2.6). Statistical analysis was performed in Microsoft Excel or Prism v6 (GraphPad Software Inc. La Jolla, CA, USA).

RESULTS AND DISCUSSION

Optimization of chromatographic separation and NESI signal intensity

The main goal in developing the IP-UHPLC/SRM-MS method was to achieve increased sensitivity for most metabolites and good chromatographic separation for the isobaric or isomeric

Table 1. Parent (Q1) and product ions (Q3), collision energies (CE) and internal standards (ISTDs) for 60 cellular metabolites that were analyzed

#	Metabolite	Q1 (*m*/*z*)	Q3 (*m*/*z*)	CE (V)	RT (min)	ISTD
1	glutamine	145	127	15	1.7	[$^{13}C_5$,$^{15}N_2$]-glutamine
2	serine	104	74	18	1.8	[$^{13}C_3$,^{15}N]-serine
3	aspartate	132	88	15	4.6	[$^{13}C_4$,^{15}N]-aspartate
4	glutamate	146	128	13	4.7	[$^{13}C_5$,^{15}N]-glutamate
5	hexosamine 6-phosphate	258	79	40	4.7	[$^{13}C_3$]-lactate
6	hydroxybutyrate	103	59	20	5.1	[$^{13}C_3$]-lactate
7	ribulose 5-phosphate	229	79	40	5.2	[$^{13}C_4$]-succinate
8	lactate	89	43	15	5.4	[$^{13}C_3$]-lactate
9	glyceraldehyde 3-phosphate	169	79	40	5.6	[$^{13}C_4$]-succinate
10	glucose 6-phosphate	259	97	20	5.9	[$^{13}C_6$]-glucose 6-phosphate
11	fructose 6-phosphate	259	97	20	5.9	[$^{13}C_6$]-glucose 6-phosphate
12	GSH	306	143	20	5.9	GSH ([$^{13}C_2$,^{15}N]-glycine)
13	erythrose 4-phosphate	199	97	25	6	[$^{13}C_4$]-succinate
14	ribose 5-phosphate	229	79	40	6	[$^{13}C_4$]-succinate
15	mevalonate	147	59	15	6.1	[$^{13}C_4$]-succinate
16	sedoheptulose 7-phosphate	289	79	40	6.1	[$^{13}C_4$]-succinate
17	glucose 1-phosphate	259	97	20	6.2	[$^{13}C_6$]-glucose 6-phosphate
18	dihydroxyacetone phosphate	169	97	20	6.8	[$^{13}C_4$]-succinate
19	phosphoserine	184	79	40	7.1	[$^{13}C_4$]-succinate
20	AMP	346	134	40	7.2	[$^{13}C_4$]-succinate
21	malate	133	115	17	7.7	[$^{13}C_4$]-succinate
22	GSSG	611	306	25	7.8	GSSG ([$^{13}C_2$,^{15}N]-glycine)
23	alpha-ketoglutarate	145	101	12	7.9	[$^{13}C_4$]-succinate
24	2-hydroxyglutarate	147	129	25	7.9	[$^{13}C_4$]-succinate
25	fumarate	115	71	15	8	[$^{13}C_4$]-fumarate
26	succinate	117	73	15	8	[$^{13}C_4$]-succinate
27	phosphohydroxypyruvate	183	79	40	10.8	[$^{13}C_4$]-succinate
28	glucose 6-P-PZ	349	79	40	13.8	[$^{13}C_6$]-glucose 6-phosphate-PZ
29	mannose 6-P-PZ	349	79	40	14.5	[$^{13}C_6$]-glucose 6-phosphate-PZ
30	ribulose 5-phosphate-PZ	319	97	40	14.8	[$^{13}C_6$]-glucose 6-phosphate-PZ
31	2-phosphoglycerate	185	79	40	15	[$^{13}C_6$]-citrate
32	ADP	426	328	20	15.1	[$^{13}C_6$]-citrate
33	phosphoenolpyruvate	167	79	40	15.4	[$^{13}C_6$]-citrate
34	citrate	191	111	15	15.4	[$^{13}C_6$]-citrate
35	ribose 5-phosphate-PZ	319	97	40	15.6	[$^{13}C_6$]-glucose 6-phosphate-PZ
36	fructose 6-P-PZ	349	79	40	15.6	[$^{13}C_6$]-glucose 6-phosphate-PZ
37	isocitrate	191	73	20	15.8	[$^{13}C_6$]-citrate
38	fructose 1,6-bisphosphate	339	97	20	15.9	[$^{13}C_6$]-citrate
39	GTP	522	424	20	15.9	[$^{13}C_6$]-citrate
40	CTP	482	384	20	16	[$^{13}C_6$]-citrate
41	6-phosphogluconate	275	97	20	16.1	[$^{13}C_6$]-citrate
42	UTP	483	385	20	16.1	[$^{13}C_6$]-citrate
43	ATP	506	159	40	16.3	[$^{13}C_6$]-citrate
44	glyceraldehyde 3-phosphate-PZ	259	79	40	17.2	[$^{13}C_6$]-glucose 6-phosphate-PZ
45	dihydroxyacetone phosphate-PZ	259	79	40	17.2	[$^{13}C_6$]-glucose 6-phosphate-PZ
46	sedoheptulose 7-phosphate-PZ	379	79	40	17.2	[$^{13}C_6$]-glucose 6-phosphate-PZ
47	erythrose 4-phosphate-PZ	289	79	40	17.6	[$^{13}C_6$]-glucose 6-phosphate-PZ
48	fructose 1,6-bisphosphate-PZ	429	79	40	18.4	[$^{13}C_6$]-glucose 6-phosphate-PZ
49	flavin adenine dinucleotide (FAD)	290	247	20	18.7	[$^{13}C_6$]-citrate
50	pyruvate-PZ	177	92	15	19.3	[$^{13}C_3$]-pyruvate-PZ
51	succinyl-CoA	866	408	40	19.4	[$^{13}C_6$]-citrate
52	acetoacetate-PZ	191	92	15	19.5	[$^{13}C_3$]-pyruvate-PZ
53	oxaloacetate-PZ	221	92	15	19.5	[$^{13}C_3$]-pyruvate-PZ
54	alpha-ketoglutarate-PZ	235	92	15	19.5	[$^{13}C_3$]-pyruvate-PZ
55	acetyl-CoA	808	408	40	19.6	[$^{13}C_6$]-citrate
56	NAD+	662	540	20	6.1*	[$^{13}C_4$]-succinate
57	NADH	664	408	30	9.4*	[$^{13}C_6$]-citrate
58	NADP+	742	620	20	9.8*	[$^{13}C_6$]-citrate
59	NADPH	774	408	40	12.2*	[$^{13}C_6$]-citrate

PZ: phenylhydrazone derivatives.
*Indicates the retention times obtained from gradient 2.

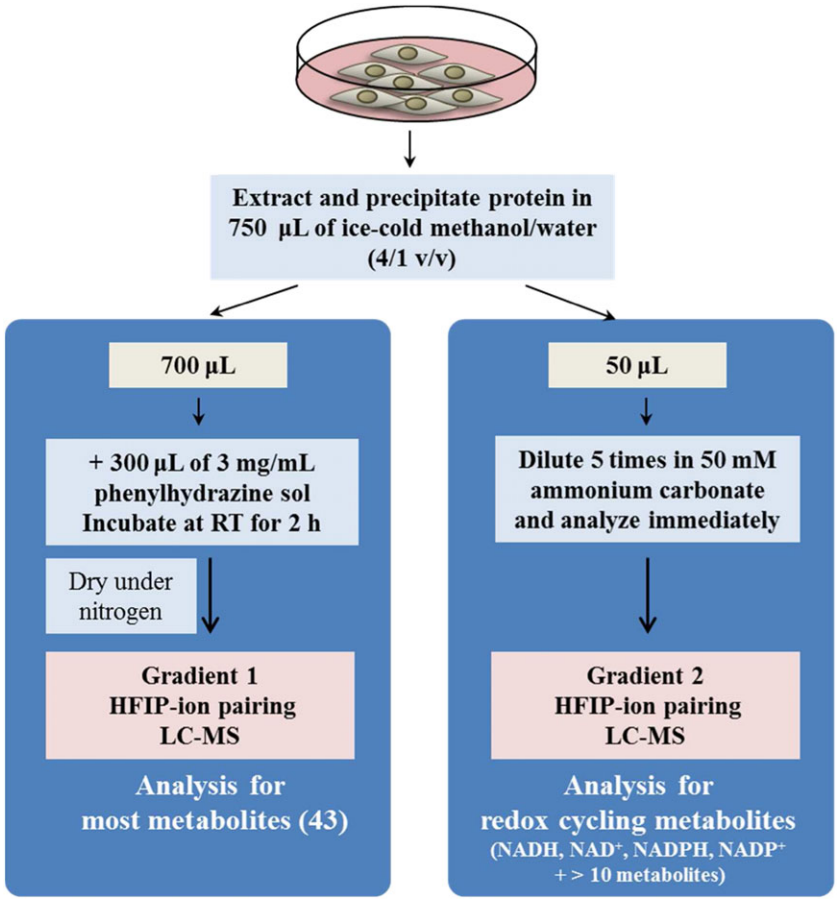

Figure 2. Work-up flow for the extraction and analysis of polar metabolites by IP-RP-UHPLC/NESI-MS for DLCL2 cells. Gradient 1 is 25 min whereas gradient 2 is 15 min in order to quickly analyze unstable redox cycling metabolites.

compounds. Here we tested phosphate and carboxylate metabolites from central energy metabolism, which are important in studies such as cancer cell metabolism. The most intense ion for all the carboxylic acids, sugar phosphates and nucleotides corresponded to the loss of a proton from each molecule $[M–H]^-$ (Table 1) as reported previously for ESI.[38] In the presence of HFIP, the product ion with least background for the sugar phosphates was 79 Da ($[PO_3]^-$). The loss of 97 Da was also monitored and used as a qualifier. All carboxylic acids gave decarboxylation products (loss of 44 Da) or decarboxylation with loss of water. The most abundant product ion from nucleotides was generated from the loss of phosphate (loss of 98 Da) or the loss of both phosphates and sugar moiety (Table 1). In the second case, the product ion is the remaining nucleobase (e.g. adenine, 134 Da).

We reasoned that the same stationary phases used in achieving good separations with IP methods previously reported[9,24–26] should also be useful with HFIP. Tributylamine (TBA) has been used previously as one of the IP reagents for the separation of small polar metabolites.[23,25,28,29,36] It is often used in combination with acetic acid[9,25] to separate carboxylic acids, sugar phosphates, and nucleotides. We expected that, compared with acetic acid, HFIP would improve the MS sensitivity, since the boiling point of the HFIP (58.2°C) is much lower than the boiling point of acetic acid (118°C). The HFIP evaporates more rapidly in the heated source than acetic acid, increasing the pH and facilitating negative ionization (Fig. 1). TBA is commonly used as an IP reagent at a concentration of 10 mM.[9,11] However, this high concentration can only be reached with lower pH when TBA is paired with a stronger acid, like acetic acid. DIPEA has higher water solubility and allows up to 10 mM concentrations when paired with HFIP in aqueous mobile phases. Therefore, we tested DIPEA and TBA on four different columns with different stationary phases from different manufacturers with different concentrations of HFIP (data not shown). Compared to DIPEA, TBA increased the retention time of the analytes by 5–10 min. Most isomers (like isocitrate/citrate and glucose 6-phosphate/fructose 6-phosphate) were not baseline separated by the increased retention times. In contrast, DIPEA provided a faster chromatographic method that still achieved separation of most of the isomeric species. As with all the parameters for IP-based methods, there is no perfect IP base for all metabolites. Due to a solubility issue of TBA in water, the combination of TBA and HFIP can never create an ideal gradient for separating all metabolites. TBA had generally less sensitivity for most metabolites. For lactate, for example, the sensitivity was 10-fold less. For most metabolites, TBA-containing mobile phases were between 2–5-fold less sensitive, but for fumarate and malate, they were approximately twice as sensitive and the peak shapes were

significantly better. Interestingly, a concentration of 1 mM DIPEA gave the best sensitivity for pure standards. However, this low concentration was insufficient for cell extracts because some metabolites were not adequately retained on the column. 5 mM DIPEA improved the retention of all of the analytes on the column and showed the highest retention time stability for running samples for long periods of time. Under this condition, the retention time shifts of the same metabolites were within 8 s for different biological samples.

The four columns we examined are described next. (1) Phenomenex Synergy Polar-RP (150 × 2 mm i.d., 4 µm, 80 Å; Phenomenex, Torrance, CA, USA): This column has fast elution times and good separation for early eluents. It provides maximum separation for late eluents especially phenylhydrazine-derivatized metabolites. (2) Xselect HSS C18 (150 × 2.1 mm, 3.5 µm, 100 Å; Waters, Milford, MA, USA): This column is excellent for DIPEA/HFIP analysis and provides good separation of phenylhydrazine-derivatized metabolites. Although it does not separate the later eluting peaks as well as the Synergy Polar-RP, this column is more robust so that more samples can be analyzed without chromatographic degradation. (3) Atlantis T3 (150 × 1 mm, 5 µm, 100 Å; Waters, Milford, MA, USA): Peaks on this column are sharp. However, the column does not provide good separation for later eluting analytes when using DIPEA/HFIP. (4) Phenomenex Luna C_{18} (250 × 2 mm i.d., 3 µm, 100 Å; Phenomenex, Torrance, CA, USA): When using a 45 min gradient, this column provides good separation for both early and late eluting isomers, e.g. fructose 6-phosphate versus glucose 6-phosphate and phenylhydrazine-derivatized fructose 6-phosphate versus glucose 6-phosphate. However, this separation can only be accomplished using long gradients and the peaks are very wide.

Conventional IP reagents such as TBA will contaminate the LC/MS system so that cleaning procedures often involve purging with solvents over long periods of time.[23] In addition, when switching from negative to positive mode, the residual IP reagent often causes intense interfering ions that are difficult to remove. It is noteworthy that in contrast to TBA, residual DIPEA did not result in strong interfering ions when switching from negative to positive ion mode. This is probably due to a balance between its lower boiling point and higher solubility in the mobile phase. In addition, the molecular weight of DIPEA (129 Da) is lower than that of TBA (185 Da) and so the interference from DIPEA is less problematic for metabolites that give rise to ions $> m/z$ 130 in positive mode. This issue of interfering ions is of even greater concern when the IP method is used on high-resolution mass spectrometers.[18,19] With the column offline, two simple washes with 0.1% formic acid in methanol coupled with high capillary temperatures at the end of the day were found to effectively prevent the buildup of DIPEA.

HFIP at a concentration of 200 mM was found to provide the best sensitivity and robustness for the cellular extract analysis (Fig. 3). For some key metabolites, especially those with longer retention time with HFIP, HFIP increased the sensitivity by more than 10-fold compared to that of DIPEA alone, including fructose 1,6-bisphosphate (F 1,6-bP) and 6-phosphogluconate (6-PG) (Fig. 3). The two isomeric products from F 1,6-bP, glyceraldehyde 3-phosphate (GAP) and dihydroxyacetone phosphate (DHAP), were baseline separated within 7 min. The sensitivity for GAP was reported to be 100 times lower than for DHAP,[23] but with the HFIP modifier we observed the sensitivity for GAP to be only 10 times less than the sensitivity for DHAP. Interestingly, compared to acetic acid, HFIP added to DIPEA significantly improved the peak shapes and increased sensitivity by 10-fold for analytes eluting towards the middle and the end of the chromatogram.

A short chromatographic method is essential in order to accommodate the analysis of a large number of samples, but none of the columns that were tested would separate all isomeric species in a short (under 30 min) chromatographic run. Different columns were able to separate different isomeric

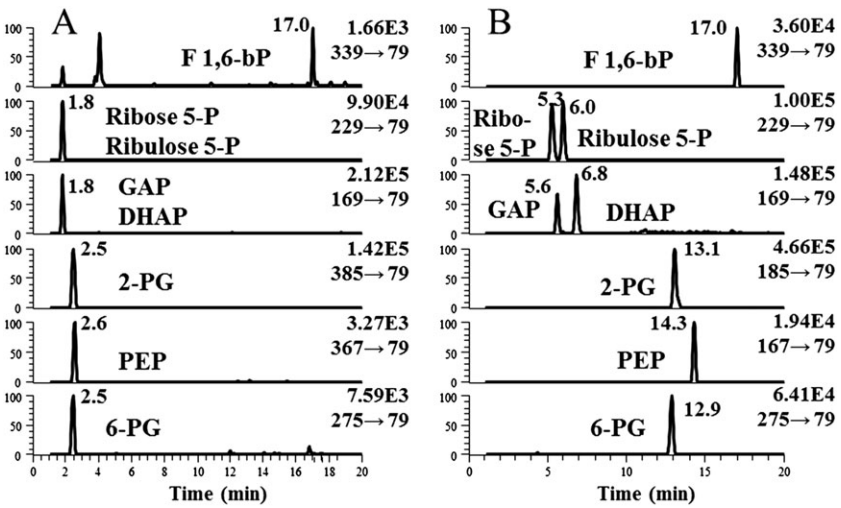

Figure 3. Representative IP-RP-UHPLC/NESI-MS chromatograms for separation improvement and sensitivity increase due to HFIP. (A) Solvents used contained 5 mM DIPEA but no HFIP. (B) Solvents used contained 5 mM DIPEA and 200 mM HFIP. F 1,6-bP: fructose 1,6-bisphosphate; GAP: glyceraldehyde 3-phosphate; DHAP: dihydroxyacetone phosphate; 2-PG: 2-phosphoglycerate; PEP: phosphoenolpyruvate.

pairs, but we found it to be extremely challenging to separate the hexose phosphates isomers. Notably, it has been challenging to separate hexose-phosphate using regular LC methods even with long gradient elutions.[25]

Derivatization of metabolites with a carbonyl group by phenylhydrazine

Many α-keto acid metabolites including pyruvate, oxaloacetate and α-ketoglutarate are unstable and difficult to analyze by LC/MS. A previous report has described the use of phenylhydrazine derivatization for analysis of α-keto acids by IP-LC/MS.[36] We have also found that phenylhydrazine derivatization stabilized the metabolites and increased their chromatographic retention times. There was also a significant enhancement in sensitivity due to the increased mass and improved chromatographic resolution. Carbohydrates exist in equilibrium between the closed ring form and the open straight-chain form. At room temperature phenylhydrazine can react with ketone or aldehyde groups from open-chain carbohydrates such as fructose 6-phosphate (F 6-P) and glucose 6-phosphate (G 6-P) to form phenylhydrazone derivatives (Fig. 4). At higher temperatures oxidation of the α-hydroxyl group occurs, which is followed by formation of a *bis*-hydrazone derivative known as an osazone.[39] UHPLC/MS analysis of reactions conducted at room temperature revealed that F 6-P, G 6-P, fructose 1,6-bisphosphate (F 1,6-bP), GAP, DHAP, ribulose 5-phosphate, ribose 5-phosphate, sedoheptulose 7-phosphate and erythrose 4-phosphate all formed mono-phenylhydrazone derivatives. Loss of the aniline radical (92 Da) or the common losses of 79 Da and 97 Da from the phenylhydrazone-phosphate provided abundant product ions. In a similar way to keto-acid phenylhydrazone derivatives, the phenylhydrazone-phosphates were retained longer on the reversed-phase column than the underivatized analytes (Table 1). Importantly, the derivatization facilitated the chromatographic separation of isomeric analytes. For example, G 6-P and F 6-P eluted at similar retention times before derivatization with phenylhydrazine (Fig. 5(A)) but were separated by more than 1 min after formation of phenylhydrazone derivatives (marked with -PZ) (Figs. 4 and 5(B)). Both analytes were also well separated from mannose 6-phosphate (Table 1). Of note, hexose phosphates including glucose 1-phosphate, mannose 1-phosphate and galactose 1-phosphate are resistant to derivatization because they cannot form open-chain keto or aldehyde forms. This further contributed to the selective detection of hexose phosphates, since underivatized hexose 1-phosphates could be monitored in the same chromatographic run. Furthermore, their analysis was not compromised by the phenylhydrazine derivatization reaction (Fig. 6). Thus, all metabolites (derivatized or not) could be quantified in a single chromatographic run.

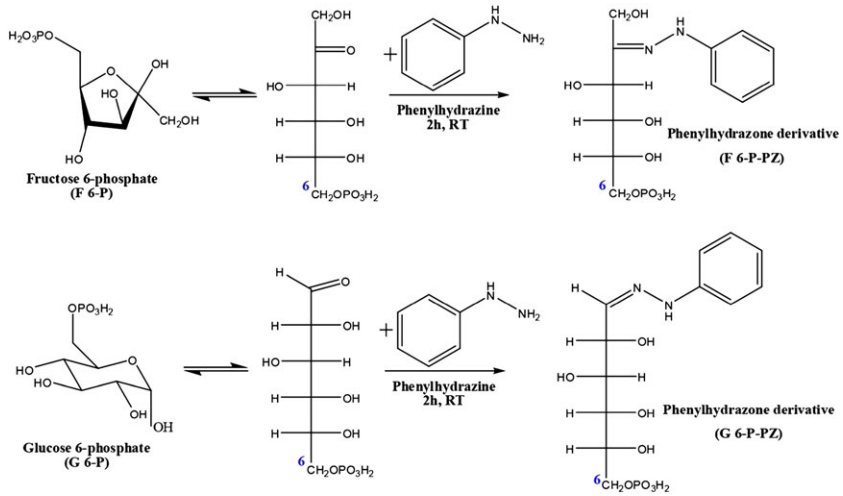

Figure 4. Derivatization of fructose 6-phosphate and glucose 6-phosphate with phenylhydrazine.

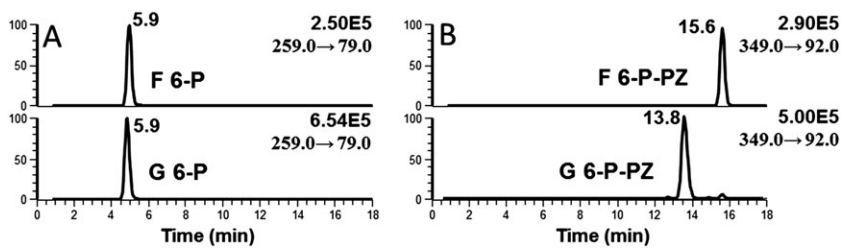

Figure 5. (A) Fructose 6-phosphate (F 6-P) and glucose 6-phosphate (G 6-P) without derivatization have identical retention times. (B) After derivatization with phenylhydrazine they are chromatographically separated by more than 1 min by IP-RP-UHPLC/NESI-MS.

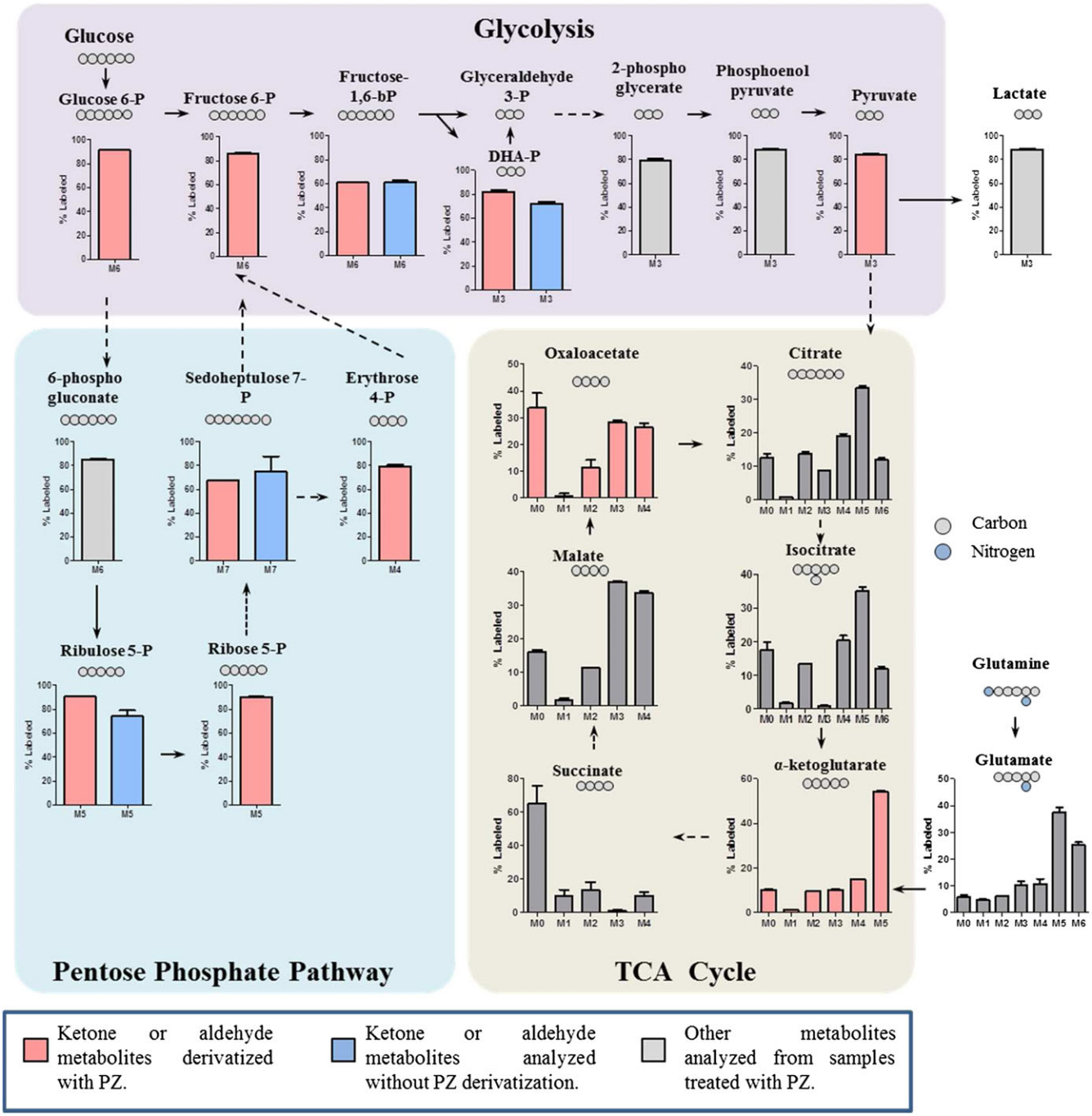

Figure 6. Quantification of isotopically labeled metabolites from DB-1 melanoma cells after derivatization with phenylhydrazine. For comparison, the carbonyl-containing metabolites were quantified in parallel experiments with phenylhydrazine (PZ) derivatization (red boxes) or without derivatization (blue boxes), using gradient 1. Metabolites without a carbonyl moiety (grey boxes) were not affected by the derivatization reaction and were quantified in the same IP-RP-UHPLC/NESI-MS analysis.

Stable isotope tracer analysis and metabolite quantification from mammalian cells

Stable isotope labeling is an important technique for dissecting metabolic pathways and analyzing metabolic fluxes by quantifying the stable isotope enrichment in metabolites from labeled nutrients.[11] To evaluate the analysis of sugar phosphates with and without phenylhydrazine derivatization using the newly developed IP-RP-UHPLC/NESI-MS method, intermediates within the central carbon metabolism were labeled by culturing DB-1 melanoma cells in glucose- and glutamine-free medium containing [$^{13}C_6$]-glucose and [$^{13}C_5$,$^{15}N_2$]-glutamine. As heavy-labeled internal standards are not available for all metabolites, this experiment aimed to verify the specific retention times for several metabolites by comparing detected isotopologue distribution with predicted isotopologue pattern. After overnight labeling, most carbons in the metabolites from glycolysis and PPP were

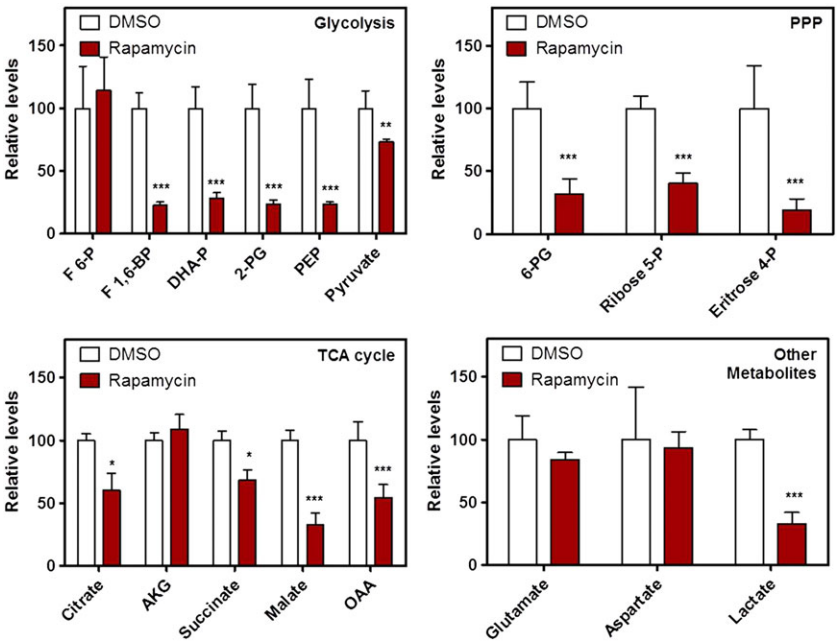

Figure 7. Levels of central energy metabolites in DLCL2 cells treated with rapamycin. The amounts of metabolites were normalized first to cell number and then to the relevant metabolites in DMSO controls. 6-PG: 6-phosphogluconate; AKG: α-ketoglutarate; OAA: oxaloacetate.

labeled. The TCA cycle metabolites had a different distribution of isotopologues (Fig. 6). For example, α-ketoglutarate had >90% labeling in M + 5, which is likely derived from [$^{13}C_5$,$^{15}N_2$]-glutamine (Fig. 6). In contrast, citrate has around 30% labeling in M + 5, which could arise from [$^{13}C_5$,$^{15}N_2$]-glutamine through reductive metabolism, whereas the 20% labeling in M + 4 may be derived from both [$^{13}C_6$]-glucose and [$^{13}C_5$,$^{15}N_2$]-glutamine through an oxidative pathway. Citrate was also detected as M + 2 (first Krebs cycle round) and M + 4 (second Krebs cycle round) from [$^{13}C_6$]-glucose, since acetyl-CoA is formed as M + 2 from [$^{13}C_6$]-glucose (Fig. 6). Reductive glutaminolysis is rare under most metabolic conditions but would increase to higher percentage in hypoxia conditions in the presence of inhibitors of mitochondrial enzymes. Of note, in terms of cellular metabolite analysis, signal/noise ratio for labeled and unlabeled metabolites was significantly higher for phenylhydrazone derivatives when compared with non-derivatized metabolites, resulting in less variation and more accurate measurements (Fig. 6, sedoheptulose 7-phosphate and ribulose 5-phosphate). We have successfully used the method to identify metabolic targets of anti-cancer drugs, to compare metabolic features of different tumor tissues, and to build network models for metabolic fluxes.[11,40] Although the detection of specific metabolites depends on the cell line and tissue used, this method provides detection of a wide range of analytes from central energy metabolites from cells, tissues and serum when limited amounts are available.

The most common approach for metabolic analysis is to analyze the levels of steady-state metabolites. Metabolic profiling covering a wide spectrum of cellular metabolites can quickly reveal pathways affected by drug treatment or different biological conditions. The methodology was also used to quantify metabolites from DLCL2 cells treated with rapamycin (Fig. 7). Rapamycin inhibits the mechanistic target of the rapamycin (mTOR) signaling pathway, which is a master regulator of cellular metabolism. Consistent with previous studies,[41,42] levels of metabolites from glycolysis and PPP were significantly decreased in rapamycin-treated cells and intermediates in the TCA cycle also decreased to a lesser extent (Fig. 7). Interestingly, intracellular glutamate and aspartate levels were the same in the presence and absence of rapamycin, which may be due to increased uptake from the medium (Fig. 7).

CONCLUSIONS

The results of metabolite quantification and stable isotope tracer analysis confirmed that the IP-RP-UHPLC/NESI-MS method was robust and accurate. NESI sensitivity was increased by the use of HFIP as the counter-ion, and phenylhydrazone derivatization facilitated the separation of isomeric metabolites as well as stabilizing α-keto acid metabolites. This derivatization procedure did not affect analysis of those metabolites that were unable to form open-chain ketone or aldehyde forms, thus allowing the multiplexed measurement of derivatized and non-derivatized analytes from the same sample.

The IP-RP-UHPLC/NESI-MS method provides accurate analysis of metabolites in cellular central energy metabolism and, especially when coupled with stable isotope tracing, gives insight into the mechanisms that are involved in metabolic adaptations.[43] A limited number of major metabolites, based on their relative abundance in normal cellular state, were evaluated in the present study. IP-RP-UHPLC/NESI-MS analyses were conducted on the most common isomeric species such as G 6-P-PZ and F 6-P-PZ, which could be separated within 25 min. However, the number of analytes quantified in a chromatographic run

could be expanded to include more metabolites from other metabolic pathways as well. The robustness of reversed-phase separation is ideal for scheduled SRM analyses based on the relative retention times, thus preserving sensitivity of analysis when multiplexing additional analytes. For high-resolution instruments[18,19] the ability of this method to chromatographically separate a wide diversity of analytes may be quite useful in quantifying a larger number of metabolites without any loss in sensitivity or specificity from isomeric or unstable species. This method will significantly facilitate metabolic research on cancer, metabolic diseases, and immune cell regulation.

Acknowledgements

This project was supported by NIH grants U54HL117798, P42ES023720, P30ES013508, P30CA016520, K22ES26235, T32ES019851, R01CA129544, and R01CA172820 and a Pennsylvania Department of Health CURE grant to NWS.

REFERENCES

[1] S. K. Grebe, R. J. Singh. LC-MS/MS in the clinical laboratory – Where to from here? *Clin. Biochem. Rev.* **2011**, *32*, 5.
[2] R. King, R. Bonfiglio, C. Fernandez-Metzler, C. Miller-Stein, T. Olah. Mechanistic investigation of ionization suppression in electrospray ionization. *J. Am. Soc. Mass Spectrom.* **2000**, *11*, 942.
[3] R. Bonfiglio, R. C. King, T. V. Olah, K. Merkle. The effects of sample preparation methods on the variability of the electrospray ionization response for model drug compounds. *Rapid Commun. Mass Spectrom.* **1999**, *13*, 1175.
[4] C. H. Chang, E. L. Pearce. Emerging concepts of T cell metabolism as a target of immunotherapy. *Nat. Immunol.* **2016**, *17*, 364.
[5] D. S. Wishart. Emerging applications of metabolomics in drug discovery and precision medicine. *Nat. Rev. Drug Discov.* **2016**. DOI: 10.1038/nrd.2016.32.
[6] L. Galluzzi, O. Kepp, M. G. Vander Heiden, G. Kroemer. Metabolic targets for cancer therapy. *Nat. Rev. Drug Discov.* **2013**, *12*, 829.
[7] J. Fan, J. Ye, J. J. Kamphorst, T. Shlomi, C. B. Thompson, J. D. Rabinowitz. Quantitative flux analysis reveals folate-dependent NADPH production. *Nature* **2014**, *510*, 298.
[8] J. Zhang, J. Fan, S. Venneti, J. R. Cross, T. Takagi, B. Bhinder, H. Djaballah, M. Kanai, E. H. Cheng, A. R. Judkins, B. Pawel, J. Baggs, S. Cherry, J. D. Rabinowitz, C. B. Thompson. Asparagine plays a critical role in regulating cellular adaptation to glutamine depletion. *Mol. Cell.* **2014**, *56*, 205.
[9] J. M. Buescher, M. R. Antoniewicz, L. G. Boros, S. C. Burgess, H. Brunengraber, C. B. Clish, R. J. DeBerardinis, O. Feron, C. Frezza, B. Ghesquiere, E. Gottlieb, K. Hiller, R. G. Jones, J. J. Kamphorst, R. G. Kibbey, A. C. Kimmelman, J. W. Locasale, S. Y. Lunt, O. D. Maddocks, C. Malloy, C. M. Metallo, E. J. Meuillet, J. Munger, K. Noh, J. D. Rabinowitz, M. Ralser, U. Sauer, G. Stephanopoulos, J. St-Pierre, D. A. Tennant, C. Wittmann, M. G. Vander Heiden, A. Vazquez, K. Vousden, J. D. Young, N. Zamboni, S. M. Fendt. A roadmap for interpreting (13)C metabolite labeling patterns from cells. *Curr. Opin. Biotechnol.* **2015**, *34*, 189.
[10] C. A. Lewis, S. J. Parker, B. P. Fiske, D. McCloskey, D. Y. Gui, C. R. Green, N. I. Vokes, A. M. Feist, M. G. Vander Heiden, C. M. Metallo. Tracing compartmentalized NADPH metabolism in the cytosol and mitochondria of mammalian cells. *Mol. Cell.* **2014**, *55*, 253.
[11] L. Guo, A. A. Shestov, A. J. Worth, K. Nath, D. S. Nelson, D. B. Leeper, J. D. Glickson, I. A. Blair. Inhibition of Mitochondrial Complex II by the Anticancer Agent Lonidamine. *J. Biol. Chem.* **2016**, *291*, 42.
[12] N. V. Rajeshkumar, P. Dutta, S. Yabuuchi, R. F. de Wilde, G. V. Martinez, A. Le, J. J. Kamphorst, J. D. Rabinowitz, S. K. Jain, M. Hidalgo, C. V. Dang, R. J. Gillies, A. Maitra. Therapeutic targeting of the Warburg effect in pancreatic cancer relies on an absence of p53 function. *Cancer Res.* **2015**, *75*, 3355.
[13] P. Kucharzewska, H. C. Christianson, M. Belting. Global profiling of metabolic adaptation to hypoxic stress in human glioblastoma cells. *PLoS One* **2015**, *10*, e0116740.
[14] C. Wang, H. Zhu, W. Zhang, F. Song, Z. Liu, S. Liu. Second-tier test for quantification of underivatized amino acids in dry blood spot for metabolic diseases in newborn screening. *Amino Acids* **2013**, *44*, 661.
[15] R. Morand, M. Donzelli, M. Haschke, S. Krahenbuhl. Quantification of plasma carnitine and acylcarnitines by high-performance liquid chromatography-tandem mass spectrometry using online solid-phase extraction. *Anal. Bioanal. Chem.* **2013**, *405*, 8829.
[16] J. Kolmert, B. Forngren, J. Lindberg, J. Ohd, K. M. Aberg, G. Nilsson, T. Moritz, A. Nordstrom. A quantitative LC/MS method targeting urinary 1-methyl-4-imidazoleacetic acid for safety monitoring of the global histamine turnover in clinical studies. *Anal. Bioanal. Chem.* **2014**, *406*, 1751.
[17] M. Yuan, S. B. Breitkopf, X. Yang, J. M. Asara. A positive/negative ion-switching, targeted mass spectrometry-based metabolomics platform for bodily fluids, cells, and fresh and fixed tissue. *Nat. Protocols* **2012**, *7*, 872.
[18] X. Liu, Z. Ser, A. A. Cluntun, S. J. Mentch, J. W. Locasale. A strategy for sensitive, large scale quantitative metabolomics. *J. Vis. Exp.* **2014**, *87*, 51358.
[19] X. Liu, Z. Ser, J. W. Locasale. Development and quantitative evaluation of a high-resolution metabolomics technology. *Anal. Chem.* **2014**, *86*, 2175.
[20] S. U. Bajad, W. Lu, E. H. Kimball, J. Yuan, C. Peterson, J. D. Rabinowitz. Separation and quantitation of water soluble cellular metabolites by hydrophilic interaction chromatography-tandem mass spectrometry. *J. Chromatogr. A* **2006**, *1125*, 76.
[21] B. Warth, G. Siegwart, M. Lemmens, R. Krska, G. Adam, R. Schuhmacher. Hydrophilic interaction liquid chromatography coupled with tandem mass spectrometry for the quantification of uridine diphosphate-glucose, uridine diphosphate-glucuronic acid, deoxynivalenol and its glucoside: In-house validation and application to wheat. *J. Chromatogr. A* **2015**, *1423*, 183.
[22] R. Joyce, V. Kuziene, X. Zou, X. Wang, F. Pullen, R. L. Loo. Development and validation of an ultra-performance liquid chromatography quadrupole time of flight mass spectrometry method for rapid quantification of free amino acids in human urine. *Amino Acids* **2016**, *48*, 219.
[23] J. M. Buescher, S. Moco, U. Sauer, N. Zamboni. Ultrahigh performance liquid chromatography-tandem mass spectrometry method for fast and robust quantification of anionic and aromatic metabolites. *Anal. Chem.* **2010**, *82*, 4403.
[24] J. M. Buscher, D. Czernik, J. C. Ewald, U. Sauer, N. Zamboni. Cross-platform comparison of methods for quantitative metabolomics of primary metabolism. *Anal. Chem.* **2009**, *81*, 2135.
[25] B. Luo, K. Groenke, R. Takors, C. Wandrey, M. Oldiges. Simultaneous determination of multiple intracellular metabolites in glycolysis, pentose phosphate pathway and

tricarboxylic acid cycle by liquid chromatography-mass spectrometry. *J. Chromatogr. A* **2007**, *1147*, 153.
[26] J. H. Huck, E. A. Struys, N. M. Verhoeven, C. Jakobs, M. S. van der Knaap. Profiling of pentose phosphate pathway intermediates in blood spots by tandem mass spectrometry: application to transaldolase deficiency. *Clin. Chem.* **2003**, *49*, 1375.
[27] W. Lu, M. F. Clasquin, E. Melamud, D. Amador-Noguez, A. A. Caudy, J. D. Rabinowitz. Metabolomic analysis via reversed-phase ion-pairing liquid chromatography coupled to a stand alone orbitrap mass spectrometer. *Anal. Chem.* **2010**, *82*, 3212.
[28] T. Reemtsma, J. Lingott, S. Roegler. Determination of 14 monoalkyl phosphates, dialkyl phosphates and dialkyl thiophosphates by LC-MS/MS in human urinary samples. *Sci. Total Environ.* **2011**, *409*, 1990.
[29] S. S. Petropoulou, M. Petreas, J. S. Park. Analytical methodology using ion-pair liquid chromatography-tandem mass spectrometry for the determination of four di-ester metabolites of organophosphate flame retardants in California human urine. *J. Chromatogr. A* **2016**, *1434*, 70.
[30] K. Moller, U. Nilsson, C. Crescenzi. Synthesis and evaluation of molecularly imprinted polymers for extracting hydrolysis products of organophosphate flame retardants. *J. Chromatogr. A* **2001**, *938*, 121.
[31] C. Horvath, W. Melander, I. Molnar, P. Molnar. Enhancement of retention by ion-pair formation in liquid chromatography with nonpolar stationary phases. *Anal. Chem.* **1977**, *49*, 2295.
[32] T. Cecchi, P. Passamonti. Retention mechanism for ion-pair chromatography with chaotropic reagents. *J. Chromatogr. A* **2009**, *1216*, 1789.
[33] K. Bleicher, E. Bayer. Various factors influencing the signal intensity of oligonucleotides in electrospray mass spectrometry. *Biol. Mass Spectrom.* **1994**, *23*, 320.
[34] L. Gong, J. S. McCullagh. Comparing ion-pairing reagents and sample dissolution solvents for ion-pairing reversed-phase liquid chromatography/electrospray ionization mass spectrometry analysis of oligonucleotides. *Rapid Commun. Mass Spectrom.* **2014**, *28*, 339.
[35] A. Apffel, J. A. Chakel, S. Fischer, K. Lichtenwalter, W. S. Hancock. Analysis of Oligonucleotides by HPLC-Electrospray Ionization Mass Spectrometry. *Anal. Chem.* **1997**, *69*, 1320.
[36] M. Zimmermann, U. Sauer, N. Zamboni. Quantification and mass isotopomer profiling of alpha-keto acids in central carbon metabolism. *Anal. Chem.* **2014**, *86*, 3232.
[37] R. Rebane, K. Herodes. Comparison of three buffer solutions for amino acid derivatization and following analysis by liquid chromatography electrospray mass spectrometry. *J. Chromatogr. A* **2012**, *1245*, 134.
[38] M. Kotrebai, J. F. Tyson, E. Block, P. C. Uden. High-performance liquid chromatography of selenium compounds utilizing perfluorinated carboxylic acid ion-pairing agents and inductively coupled plasma and electrospray ionization mass spectrometric detection. *J. Chromatogr. A* **2000**, *866*, 51.
[39] E. Fischer. Schmelzpunkt des Phenylhydrazins und einiger Osazone. *Ber. Dtsch. Chem. Ges.* **1908**, *41*, 73.
[40] A. A. Shestov, A. Mancuso, S. C. Lee, L. Guo, D. S. Nelson, J. C. Roman, P. G. Henry, D. B. Leeper, I. A. Blair, J. D. Glickson. Bonded cumomer analysis of human melanoma metabolism monitored by ^{13}C NMR spectroscopy of perfused tumor cells. *J. Biol. Chem.* **2016**, *291*, 5157.
[41] P. Tucci, G. Porta, M. Agostini, A. Antonov, A. V. Garabadgiu, G. Melino, A. E. Willis. Rapamycin regulates biochemical metabolites. *Cell Cycle* **2013**, *12*, 2454.
[42] A. Ramanathan, S. L. Schreiber. Direct control of mitochondrial function by mTOR. *Proc. Natl. Acad. Sci. USA* **2009**, *106*, 22229.
[43] F. Tang, K. Wu, Z. Nie, L. Ding, Q. Liu, J. Yuan, M. Guo, S. Yao. Quantification of amino acid ionic liquids using liquid chromatography-mass spectrometry. *J. Chromatogr. A* **2008**, *1208*, 175.

